

Sea ice outlook in 2013: Summer atmospheric and sea ice dynamical contributions to fall sea ice extent

July Update

M.G. Asplin, J.V. Lukovich, B. Horton, M. Ogi, and D.G. Barber
Centre for Earth Observation Science (CEOS)
University of Manitoba, Winnipeg, Canada

Estimate for sea ice extent for September, 2013; comparable to or slightly less than the 2007 minimum in sea ice extent, or 4.0 +/- 0.25 million square kilometers.

Executive Summary

The mean ice concentration anomaly for June 2013 is $0.9 \times 10^6 \text{ km}^2$ greater than June 2012, however Arctic sea ice thicknesses and volumes continue to remain the lowest on record. Anomalous cyclonic atmospheric circulation throughout the Arctic Basin during June has continued to precondition sea ice, making the ice cover vulnerable to a precipitous drop in sea ice extent; however the persistence of the June cyclonic circulation (and cloudiness associated with the surface lows) has induced divergence within the sea ice cover, and has delayed the onset of the rapid sea ice extent decline typically observed in June. Given the preconditioned ice cover, and short-term forecast for increased high pressure in the Arctic, it is still likely that the 2013 fall sea ice extent will achieve values comparable to those of 2007. We see July as a critical month where favorable atmospheric and oceanic conditions could rapidly erode the preconditioned Arctic sea ice cover.

Rationale

June 2013 has continued to exhibit a complex and anomalous setup for the 2013 melt season. The mean ice concentration anomaly for June 2013 is $0.9 \times 10^6 \text{ km}^2$ greater than June 2012 (Figure 1). Wind-driven sea ice drift patterns in June have increased spatial variability of sea ice export through Fram Strait in 2013, which is in contrast to high rates of ice drift observed in 2012 (*e.g.* Figure 4). This suggests a reduction in ice export through Fram Strait in 2013 as compared to 2012. Furthermore, the Beaufort Sea ice gyre appears to continue to be responding to the persistent surface low over the Arctic. This strong cyclonic circulation pattern corresponds to strong cyclonic atmospheric conditions described in Serreze and Barret (2008). The onset and persistence of this pattern in late-May through June suggests that the 2013 sea ice minimum extent will be strongly influenced by the net contributions of cyclonic wind forcing, precipitation, and cloud radiative forcing. In particular, snowfall and cloud cover would increase regional albedo, thereby affecting solar irradiation of the sea ice surface.

Dynamic sea ice processes are important to consider this year. The widespread fracture of the winter ice cover in the Beaufort Sea in winter 2013 likely resulted in some

localized dynamic thickening within the first-year ice cover in this region. Furthermore, the observed cyclone-forced divergence of the Arctic sea ice cover has resulted in high sea ice concentrations along the coastlines. As 30 – 80% of sea ice volume in a given area can be contained in pressure ridges (*Haas, 2003*), the impacts of these dynamic forcing events on sea ice mass balance must be considered.

Discussion

Mean June sea ice extents and concentrations are contrasted between 2012 and 2013 (Figure 1). The mean ice concentration anomaly for June 2013 is $0.9 \times 10^6 \text{ km}^2$ greater than for June 2012. Most notable are the near absence of the flaw lead feature in the southern Beaufort sea in 2013, which instead contains 95%+ sea ice cover, and the absence of sea ice cover along the east Greenland coast. The Kara Sea continues to have some low concentrations of sea ice cover in 2013, compared to ice-free conditions 2012. The AMSR-2 data for 01 July 2013 (Figure 2) continues to show large areas containing 50 – 75% sea ice concentration near the North Pole, also visible in the MODIS Arctic Mosaic for 01 July 2013 (Figure 3). Fracturing of this nature was noted elsewhere in the pack ice during July 2012, and undoubtedly represents widespread fractured ice floes. These ice floes will continue to be subject to wind forcing, lateral melting, and further mechanical fracture from wave action (*e.g. Steer et al., 2008*) and wave-induced melt (*e.g. Wadhams, 1979*) for the next two months.

The most striking feature of the 2013 melt season thus far is an anomalous cyclonic atmospheric circulation pattern over the Beaufort and Chukchi Sea associated with a series of persistent surface lows with high pressure anomalies over mid-latitudes (Figure 4). Furthermore, these lows appear to be coupled to an anomalously deep upper-level low, evidenced at 500hPa (figure 4). This pattern follows the findings of a well-developed cyclone pattern as described by Serreze and Barret (2008). Furthermore, they report increased propensity for precipitation over the Arctic during enhanced cyclonic circulation periods. The effects of precipitation are a key variable to consider as snowfall in late spring and early summer would increase regional albedos over sea ice, and act as a thermodynamic insulator. However, precipitation that falls as rain or freezing drizzle will not have the same effect. Sea ice in these areas will be subject to melt from ocean heat flux, warm air advection from continental locales, and solar radiation (provided that High pressure builds in). Another factor to consider is whether an Arctic Dipole anomaly, seen in recent years, is able to establish itself in July, and promote warm-air advection and clear skies over the Beaufort and Chukchi Seas.

The greater concentrations of sea ice in the Southern Beaufort are attributable to persistent surface cyclonic wind forcing and cyclonic motion on the Beaufort Sea ice gyre (Figures 4 and 5). This is evidenced by the fact that the pack ice has still not moved away from the land fast ice in Amundsen Gulf to create the typical spring flaw lead which was present in 2012 (Figure 1). A contracted, reversed Beaufort Sea ice gyre is discernible on the 01 July 2013 ice drift (Figure 5). This pattern appears to favor building sea ice concentrations in the southern Beaufort Sea. A reversed sea ice gyre can contribute to ice export along the east coast of Greenland; however, a lack of observed

ice in Fram Strait suggests that rates of ice export are presently low. Dynamic sea ice processes appear to be playing prominent episodic roles in 2013. The effects of the observed large-scale winter fracturing of the Beaufort Sea Ice Gyre during February and March of 2013 (NSIDC, 2013) on the sea ice cover continue to be of great interest (See June outlook for discussion of this event). Dynamic thickening as a result of the winter fracture event has likely been enhanced further by anomalous wind forcing of sea ice throughout June 2013. The strong cyclonic atmospheric circulation was observed to have induced divergence throughout the Arctic sea ice cover which has resulted in sea ice concentrations building along the Canadian, Alaskan and Russian coastlines for a period in June. This likely dynamically increased regional ice thicknesses and sea ice concentrations in these areas. Furthermore, total Arctic sea ice extent may have been maintained throughout June by divergent forcing of the sea ice cover. The sea ice extent (Area with at least 15% coverage as reported by NSIDC) has shown a sudden acceleration in sea ice decline during the last 10 days of June (Figure 6) which, at its present rate of decline, could potentially catch up to the 2012 sea ice extent trendline by mid-July. It remains to be seen if the cyclonically-diverged sea ice cover will

References

Haas, C.S. (2003), Dynamics vs. thermodynamics: the sea ice thickness distribution, in Thomas, D.N. and Dieckmann (eds.) *Sea Ice: An Introduction to its physics, chemistry, biology and geology*, 82 – 111, Blackwell Science, Oxford.

Serreze, Mark C., Andrew P. Barrett, 2008: The Summer Cyclone Maximum over the Central Arctic Ocean. *J. Climate*, **21**, 1048–1065.
doi: <http://dx.doi.org/10.1175/2007JCLI1810.1>

Steer, A., A. Worby, and P. Heil (2008), Observed changes in sea-ice floe distribution during early summer in the Western Weddell Sea, *Deep Sea Res., Part II*, **55**, 933 – 942, doi:10.1016/j.dsr2.2007.12.016

Wadhams, P., A. E. Gill, and P. F. Linden (1979), Transects by submarine of the East Greenland Polar Front, *Deep Sea Res.*, **26A**, 1311– 1327.

Figures

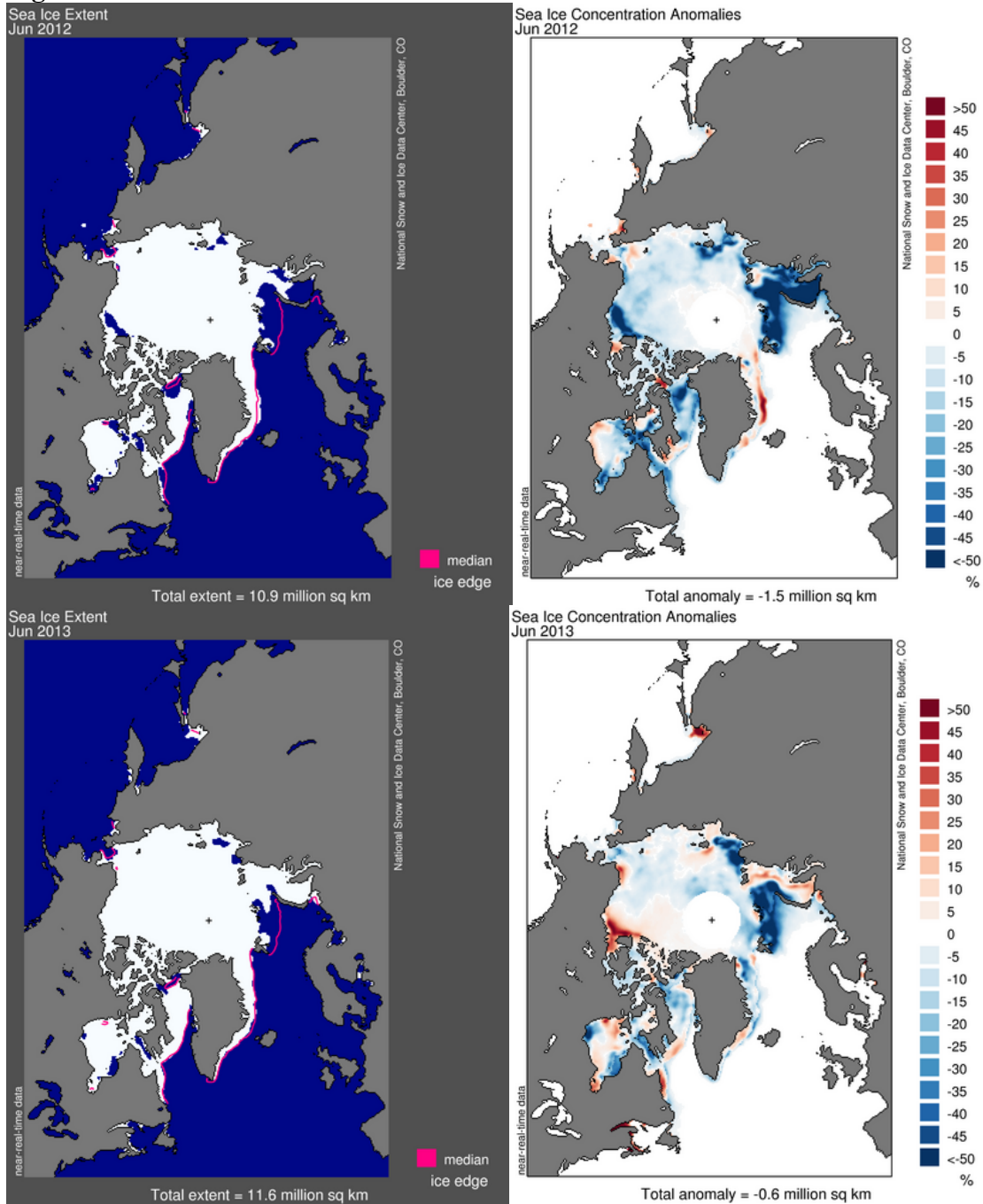


Figure 1. Mean Arctic sea ice extent for June 2012 (top left), and June 2013 (bottom left). Sea ice concentration anomalies are presented for June 2012 (top right), and June 2013 (bottom right). Images were retrieved from the National Snow and Ice Data Centre (www.NSIDC.org).

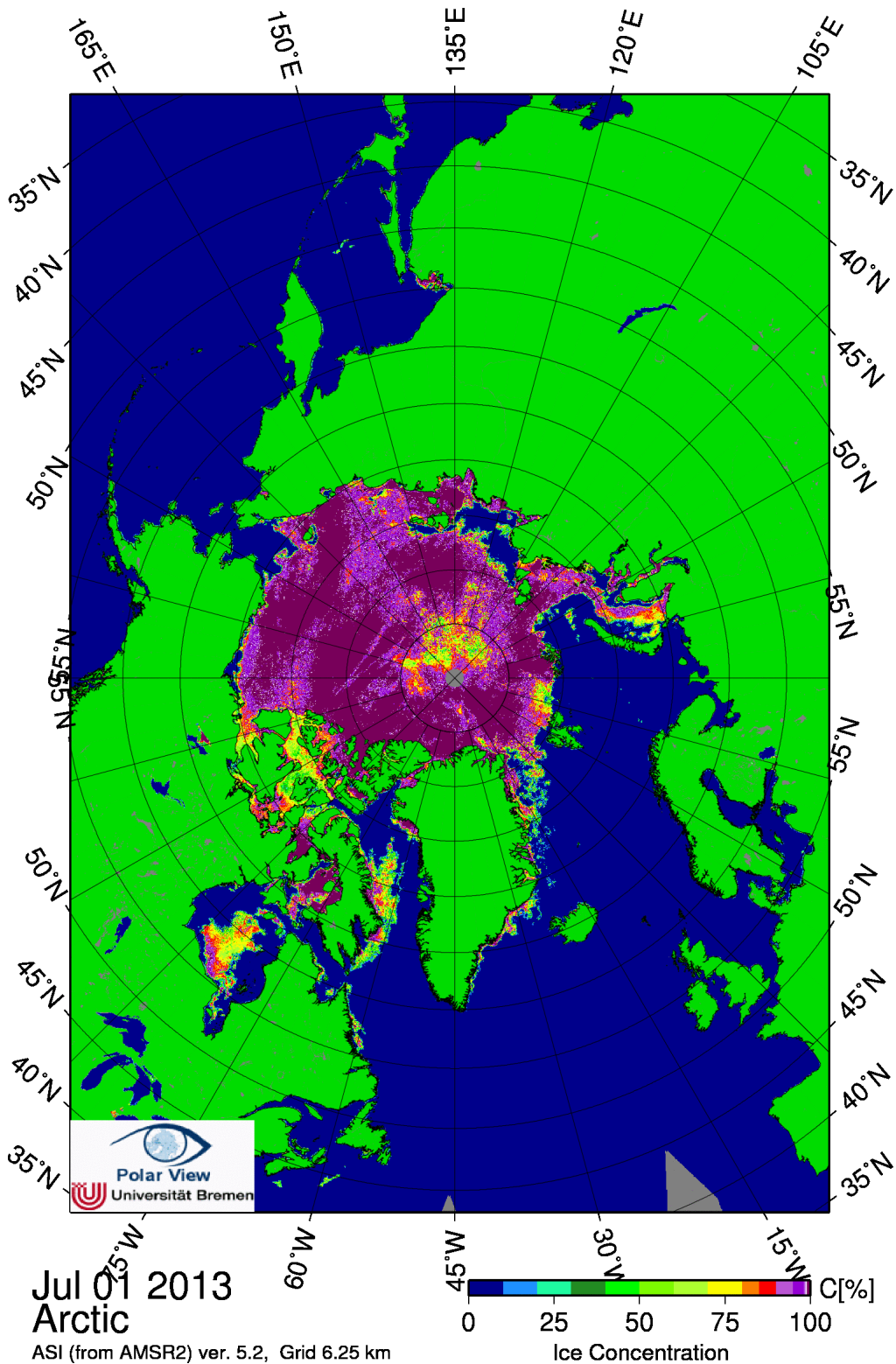


Figure 2. AMSR-2 Sea ice concentration for 01 July 2013. Image provided by the University of Bremen at <http://www.iup.uni-bremen.de:8084/ssmisdta/> (note: AMSR-2 was not yet publically available in June 2012).

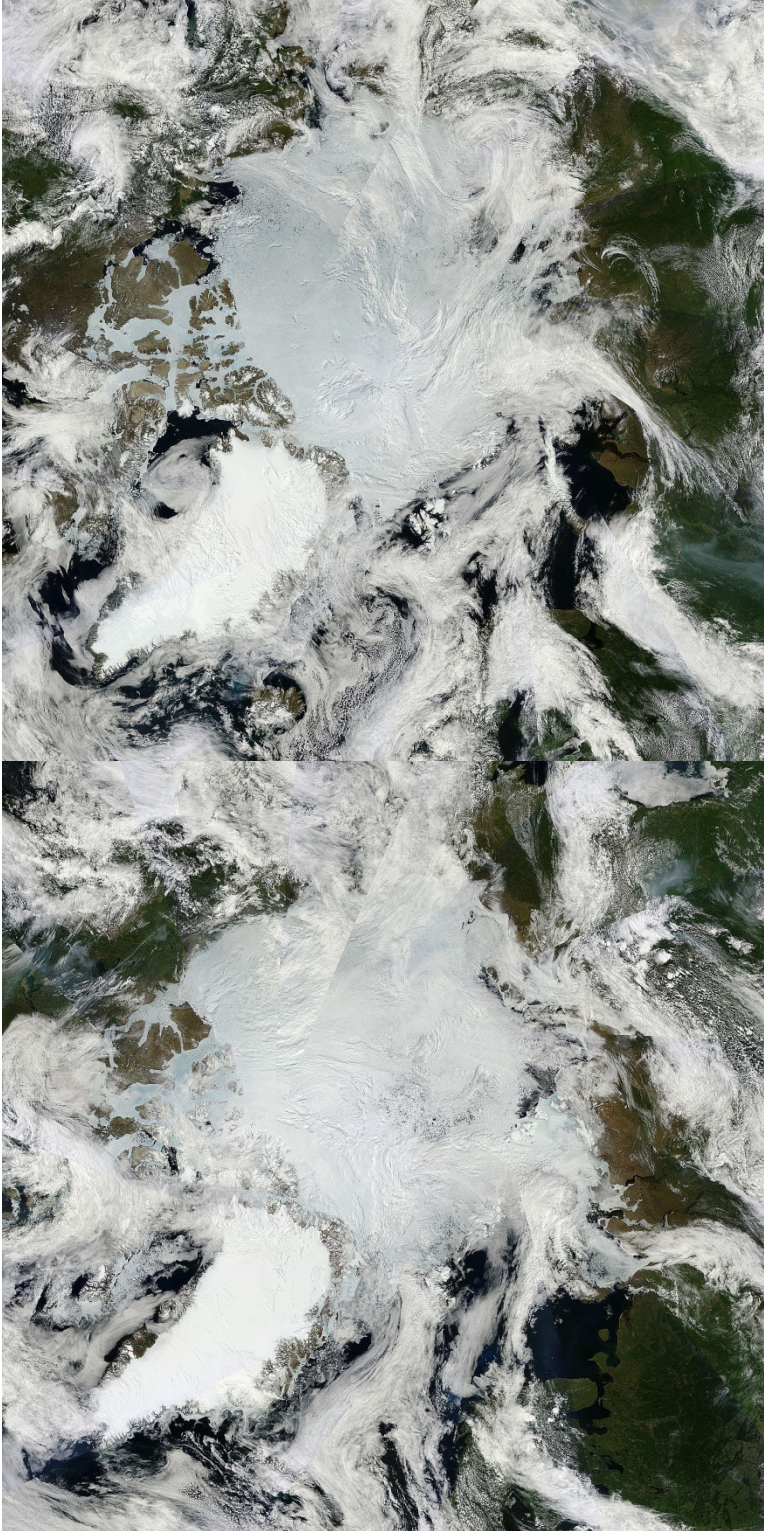


Figure 3. MODIS Terra Arctic Mosaic image for 01 July 2012 (top) and 01 July 2013 (bottom) found at: <http://rapidfire.sci.gsfc.nasa.gov/imagery/>

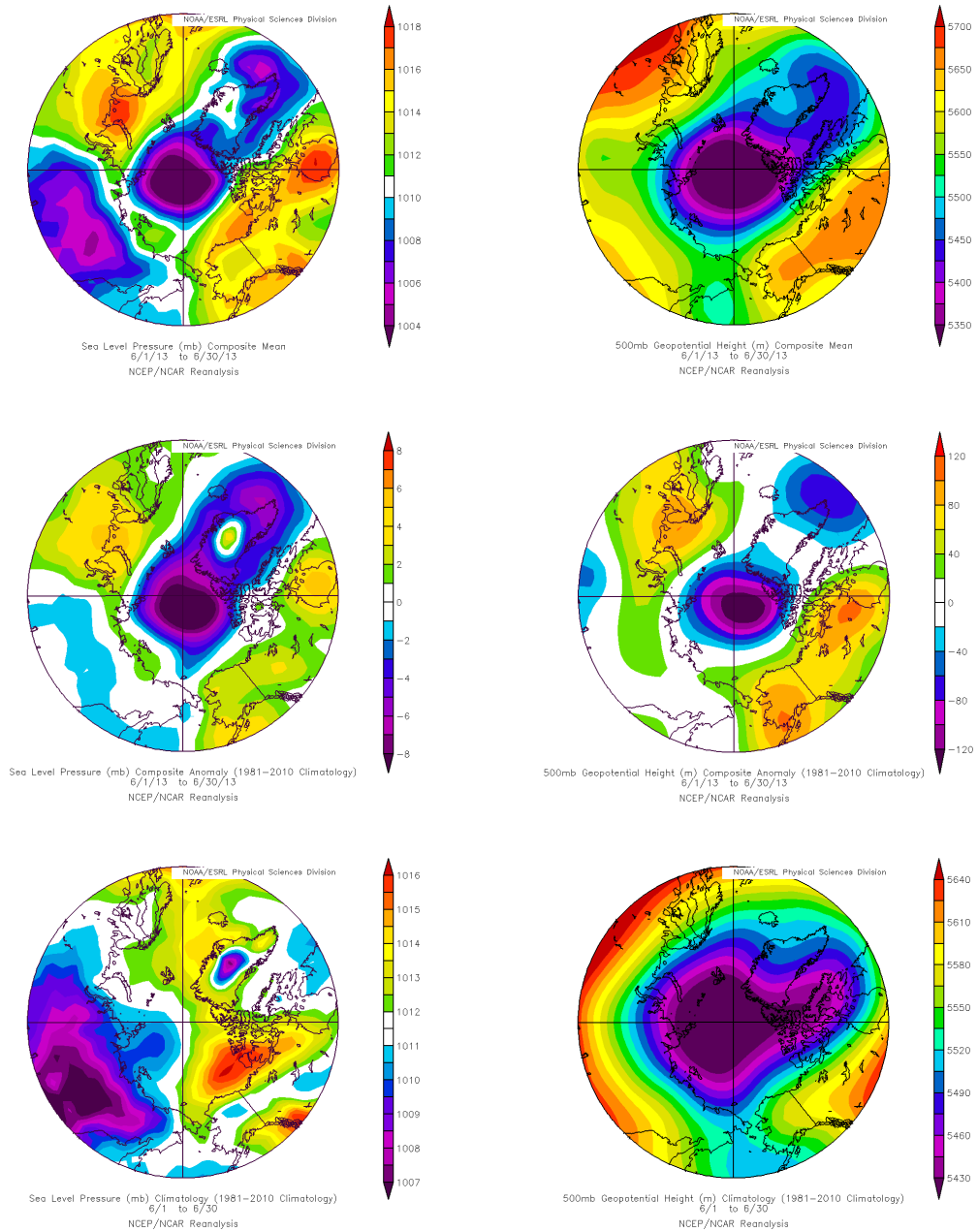


Figure 4. Left column: June 2013 mean sea level pressure (SLP) (top left), SLP anomaly (middle left), and SLP climatology for 1981 – 2010 (bottom left). Right column: June 2013 mean 500mb geopotential heights (top left), 500mb geopotential height anomalies (middle left), and 500mb geopotential heights climatology for 1981 – 2010 (bottom left). Images provided by the NOAA/ESRL Physical Sciences Division, Boulder Colorado from their Web site at <http://www.esrl.noaa.gov/psd/>.

ARCc0.08-03.5 Ice Speed and Drift: 20120701

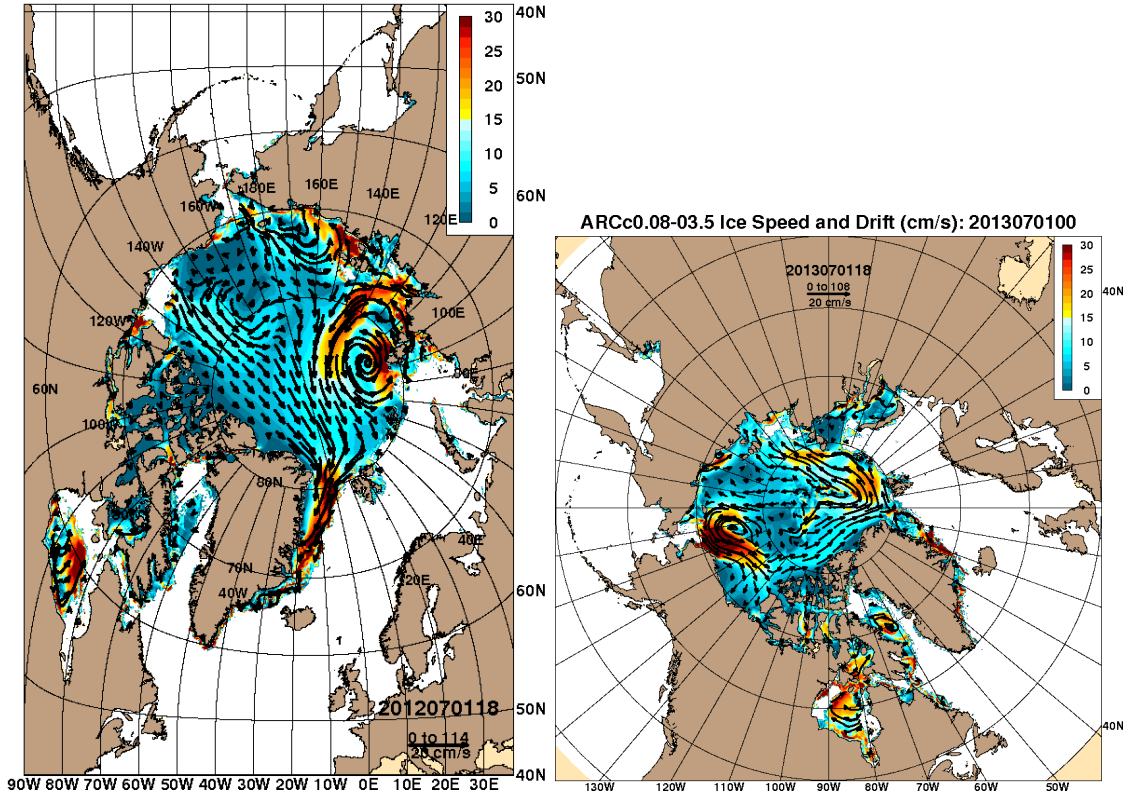


Figure 5. Nowcast ice drift images for 01 July 2012 (left), and 01 July 2013 (right). Nowcasts obtained from the Naval Research Laboratory (NRL) – HYCOM Consortium for Data-Assimilative Ocean Modeling at: <http://www7320.nrlssc.navy.mil/hycomARC/navo/arcticictn/nowcast/>.

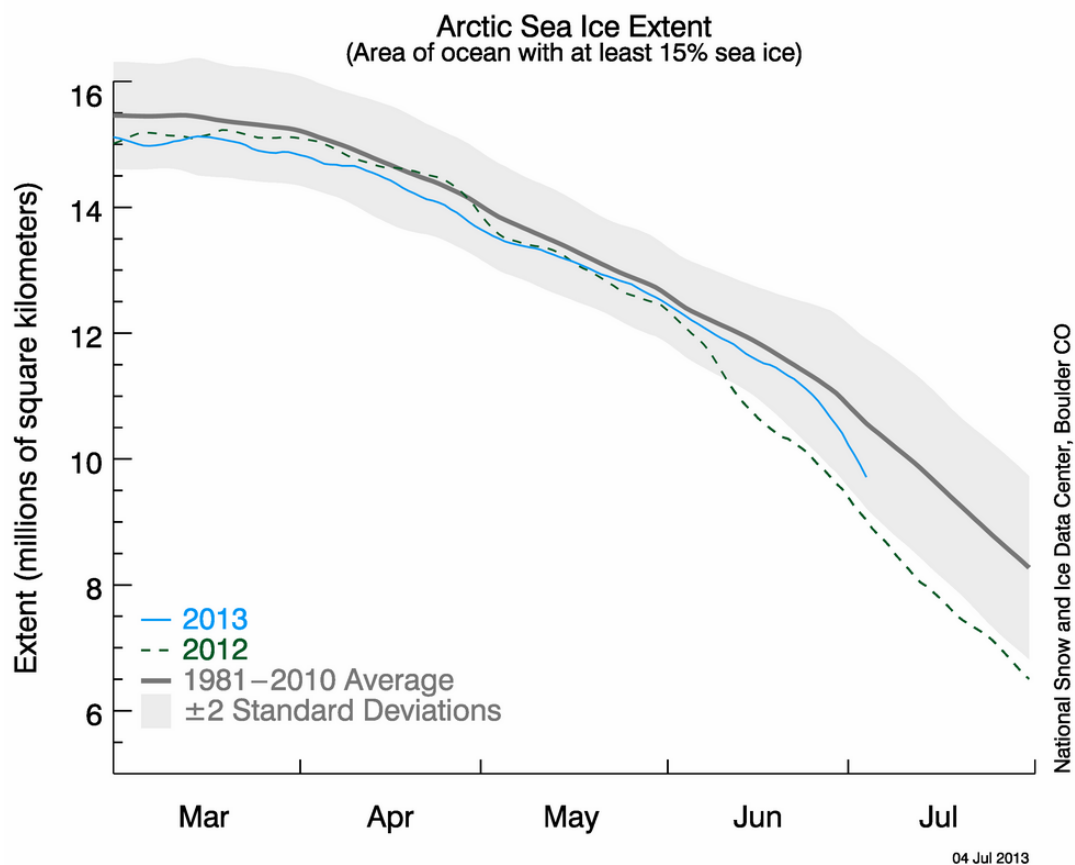


Figure 6. 05 July 2013 Arctic Sea Ice Extent (Blue line) contrasted against the 2012 extent (green line), and climatology. Image was retrieved from the National Snow and Ice Data Centre (www.NSIDC.org).